Scanning Microscopy

Volume 6 | Number 4 Article 3

10-9-1992

Investigation of Living Cells in the Nanometer Regime with the Scanning Force Microscope

J. K. H. Hörber
Max-Planck-Institut fur Medizinische Forschung

W. Häberle
Physics Group Munich

F. Ohnesorge
Physics Group Munich

G. Binnig
Physics Group Munich

H. G. Liebich
Tierarztliche Fakultat der Ludwig-Maximilians-Universitat Munchen

See next page for additional authors

Investigation of Living Cells in the Nanometer Regime with the Scanning Force Microscope

Authors

J. K. H. Hörber, W. Häberle, F. Ohnesorge, G. Binnig, H. G. Liebich, C. P. Czerny, H. Mahnel, and A. Mayr

Scanning Microscopy, Vol. 6, No. 4, 1992 (Pages 919-930) 0891-7035/92$5.00+.00
Scanning Microscopy International, Chicago (AMF O'Hare), IL 60666 USA

INVESTIGATION OF LIVING CELLS IN THE NANOMETER REGIME WITH THE SCANNING FORCE MICROSCOPE

J.K.H.Hörber[1*], W.Häberle[2], F.Ohnesorge[2], G. Binnig[2], H.G. Liebich[3], C.P.Czerny[3], H.Mahnel[3], and A.Mayr[3]

[1]Max-Planck-Institut für Medizinische Forschung, D-6900 Heidelberg, Federal Republic of Germany (FRG)
[2]IBM Research Division, Physics Group Munich, Schellingstraβe 4, 8000 München 40, FRG
[3]Tierärztliche Fakultät der Ludwig-Maximilians-Universität München,
Veterinär-straβe 13, 8000 München 22, FRG

(Received for publication August 6, 1992, and in revised form October 9, 1992)

Abstract

Membrane structures of different types of cells are imaged in the nanometer regime by scanning force microscopy (SFM). The images are compared to those obtained with a scanning electron microscope (SEM). The SFM imaging can be done on the outer cell membrane under conditions that keep the cells alive in aqueous solutions. This opens up the possibility of observing the kinematics of the structures that determine the interaction of a cell with its environment. Therefore, STM observations, together with information obtained with the electron microscope, open up new ways of studying the development of biological structures. With the currently possible resolution, the SFM gives access to processes such as antibody binding or endo- and exocytosis, including processes correlated to the infection of cells by viruses.

Key Words: Scanning force microscopy, cell surface, *Bacillus coagulans*, S-layer, erythrocytes, Concanavalin A, monkey kidney cells, pox virus, exocytosis.

***Address for correspondence:**
J.K.H. Hörber,
MPI für Med. Forschung,
Abt. Zellphysiologie,
Jahnstraβe 29,
D-6900 Heidelberg,
Federal Republic of Germany
Phone No.: +49/6221/486-463
Fax No.: +49/6221/486-459

Introduction

Scanning probe techniques, such as, scanning tunneling microscopy (STM) or scanning force microscopy (SFM), which are basically surface science instruments (Binnig *et al.*, 1982, 1986), have shown that they can be developed into powerful tools to study biological structures (Binnig *et al.*, 1984; Marti *et al.*, 1988), in particular the dynamics thereof (Drake *et al.*, 1989).

Observations with the STM of artificial lipid films (Fuchs *et al.*, 1987; Smith *et al.*, 1987) and with integrated proteins (Hörber *et al.*, 1988) demonstrated very early that even membranes might be accessible to these instruments. This was confirmed by SFM observations of lipid films (Egger *et al.*, 1990; Meyer *et al.*, 1991). Therefore, first attempts to study natural membranes (Worcester *et al.*, 1988; Guckenberger *et al.*, 1989; Jericho *et al.*, 1990; Hörber *et al.*, 1991) with SFM and STM were soon made, but showed that the reliable preparation of such membranes on substrates is quite difficult because numerous surface effects at the substrate influence preparation and imaging by introducing considerable identification problems. One way to avoid at least some of the problems at the surface of the sample is to coat it with homogeneous conducting material. Some groups tried such and other methods borrowed from electron microscopy to improve the results (Travaglini *et al.*, 1987; Stemmer *et al.*, 1987; Zasadzinski *et al.*, 1988). Nevertheless, the preparation of artificial and natural membranes on well-defined solid supports is rather difficult and it is not obvious to what extent they can actually show the normal cell membrane structures. Therefore, it is tempting to deal with whole cells and thus to make use of nature's optimized technique to stabilize membranes. In this case, of course, many problems arise from the complexity of the structure, leading again to identification problems. First attempts to investigate whole cells have been made with both techniques, the STM (Ruppersberg *et al.*, 1989; Dai *et al.*, 1991; Ito *et al.*, 1991) and the SFM (Gould *et al.*, 1990; Butt *et al.*, 1990; Kasas and Celio, 1992), using various techniques to affix the cells to a substrate.

A rather different approach to investigate cell membranes with a specially developed SFM emerged in 1989 when the first reproducible images were made of the outer membrane of a living cell, fixed only by a pipette in its normal growth medium (Häberle *et al.*, 1989). In this way, the cell can be kept alive for days while imaging. This makes studies of live activities and kinematics possible, in addition to the application of other cell physiological measuring techniques. With this step in the development of scanning probe instruments, the capability of optical microscopy to investigate the dynamics of biological processes of cell membranes under physiological conditions could be extended into the nanometer regime. But it is not this imaging capability that might be the most attractive feature of this technique in future, it is the ability to measure interaction forces that determine the dynamical processes between macromolecules that may lead to new and essential insights.

At the moment, structures as small as about 10 nm can be resolved. This gives access to processes such as the binding of labeled antibodies, endo- and exocytosis, pore formation, and the dynamics of surface structures in general. As, with the integrated tip of the SFM cantilever, forces are applied to the investigated cell membrane, the mechanical properties of cell surface structures get involved in the imaging process. On one hand, this fact mixes topographic and elastic properties of the sample in the images, while on the other hand, it provides additional information about cell membranes and their dynamics in various situations during the life of the cell, if these two aspects in the SFM images can be separated. For this, independent data are needed, such as topographic data from electron microscopy or from modulation techniques by SFM.

Material and Methods

Fig. 1a, shows the schematic arrangement of the SFM with tunneling detection above the objective of an inverted optical microscope (Nikon). The sample area can be observed from below through a planar surface defined by a glass plate with a magnification of x600-1200 and from above by a stereo microscope with a magnification of x40-200. The illumination is from the top through the less well-defined surface of the aqueous solution. In order not to block the illumination, the tunneling sensor (Scanner II) and the scanned micropipette (Scanner I) point towards the focal plane at an angle of 45°. The lever is mounted in a fixed position within the liquid slightly above the glass plate tilted by 45°. In this way, the lever is deflected in a direction parallel to the tunneling tip.

A short pipette of 0.8 mm outer diameter is pulled to about 2-4 μm on one end, in the way used for the production of patch clamp pipettes (Sakmann and Neher, 1983). It is mounted on the piezo-tube scanner and coupled to a fine and flexible Teflon tube, through which the pressure in the pipette can be adjusted by a piston or water pump. The pipette is fixed at an angle that allows imaging of the cell but without the danger of touching the pipette with the lever. All these components are located in a container of 50 μl volume. The glass plate above the objective of the optical microscope forms the bottom of this container.

Before the cells are added, the tunneling tip is brought into tunneling contact with the lever already in the solution. The electropotentials of all contacting parts have to be adjusted such that the ion current to the tip, and hopefully also the electrochemistry, are minimized. After adding several microliters of the cell suspension, a single cell can be sucked onto the pipette and fixed there by maintaining low pressure in the pipette. The other cells are removed through the pumping system. The fixed cell is placed close to the SFM lever by a rough approach with screws and finally positioned by the piezo scanner. When the cell is in close contact with the tip of the lever, scanning of the capillary with the cell attached leads to position-dependent deflections of the lever. The maximum possible scan width is 3.6 μm. The levers used are microfabricated silicon and silicon nitrite triangles with 100 μm length and with a spring constant of 0.12 N/m, and were provided courtesy of Shinya Akamine (Stanford University) and Mike Kirk (Park Scientific Instruments).

The piezo tube holding the tunneling tip is part of a feedback loop that stabilizes the tunneling current to a value in the range of 0.5-1 nA. The changes in the feedback voltage on this piezo are a measure for the deflection of the lever. This signal is used by an digital image storage (Arlunya) to create a video signal, with respect to the x,y movement of the pipette, which is recorded on video tape. Single pictures are low-pass Fourier filtered to reduce the signal noise and displayed by a Silicon Graphics Iris work station.

To increase the long-term stability of the instrument for observations of cells for many hours, we can switch to optical detection (Häberle *et al.*, 1992). For certain results, especially for experiments with the erythrocytes, the tunnel probe was used to sense the lever motion. The other results were obtained by optical detection of the lever deflection, which was sensed by measuring the deflection of a reflected laser beam with a bi-cell photodiode, as has become common practice in the SFM field. In our setup, however, no lenses are used. Instead, an optical fiber is brought very close to the lever and positioned in three dimensions by the manipulator built for the tunneling tip. This configuration is shown in Figure 1b.

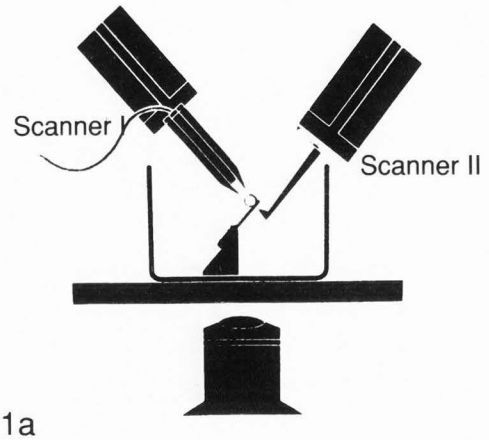

Fig.1a

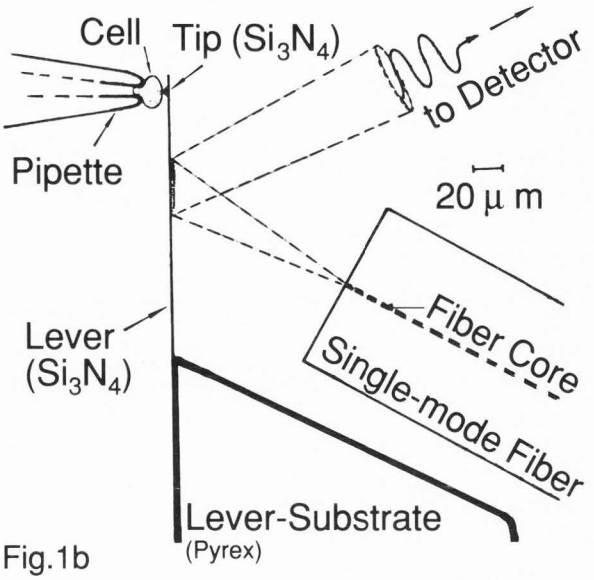

Fig.1b

Figure 1. Schematic drawing of the SFM set-up on top of a inverse optical microscope; **a**) with tunneling detection; **b**) in detail with optical detection.

The application of both detection systems to investigate a defined area of the cell surface reveals similar structures and corrugations. In both cases, the forces, as determined by the measured deflection in the constant height mode, were between 10^{-7} and 10^{-9} N for images with good contrast. This suggests that the influence of the tunneling tip on the spring constant of the lever is not very significant. The limitation in the constant height mode is the corrugation which can lead to very high forces and strong tip surface interactions.

Bacillus coagulans

Bacteria cells were placed with a drop of solution on a quartz glass slide which had previously been coated with polylysine to improve the fixation of the cells to the substrate. While imaging, the sample was kept immersed in buffer solution. The SFM used for the experiments with bacteria cells on glass slides was another home-built type of SFM described in Ohnesorge *et al.* (1992) with optical detection. The cells of *Bacillus coagulans E38-66* were provided courtesy of D. Pum (Center for Ultrastructural Research, Vienna).

Erythrocytes

Fresh human erythrocytes were used for the experiments after briefly cleaning them by washing three times with a physiological NaCl solution and concentrating them in a centrifuge at 1200 rpm for 10 minutes. The concentrate was diluted to 1:1000 before adding about 10 μl to the physiological solution in the container where the cell is observed by the SFM. Higher salt concentrations were achieved by adding grains of salt to obtain a concentration of up to 250 mM.

For the experiment of binding molecular structures to the erythrocyte surface, Concanavalin A (Sigma) was used which is not blood group specific but has an affinity for terminal mannosyl and glycosyl residues. It was labeled with 20 nm colloidal gold particles and used in mmolar concentrations

Cell cultures and virus propagation

The permanent African green monkey kidney cell line MA-104 was grown as monolayer cultures in Earl's minimal essential medium (EMEM) containing 5% fetal calf serum (FCS) and antibiotics. Stocks of the neurovirulent vaccinia virus strain Munich 1 were prepared by infecting the MA-104 cells at a multiplicity of 1 $TCID_{50}$/cell and adsorption for 60 minutes at 25 °C (Czerny *et al.*, 1989, 1990). The virus medium was EMEM with 1% FCS. One day later, a cytopathogenic effect (CPE) had developed up to 90-100 % cytolysis. The infected cultures were freeze-thawed (-70/25 °C), intensively sonicated by a Branson sonifier and centrifuged at 1,000 x g and 4 °C for 10 minutes to remove cell debris. The supernatants containing the virus were collected and used as the test virus. Infectivity titers were determined on Falcon 96-well microplates (Becton Dickinson, Heidelberg) and calculated by the 50% end-point-method of Spearman and Kaerber ($TCID_{50}$) seven days after incubation at 37 °C (Mayr *et al.*, 1974).

Results and Discussion

Structures of a bacterial cell membrane

The outer cell envelope of bacteria of the strain *Bacillus coagulans* E38-66 is formed by a regularly structured protein surface layer (S-layer). Electron micrographs of freeze-etched preparations of whole cells

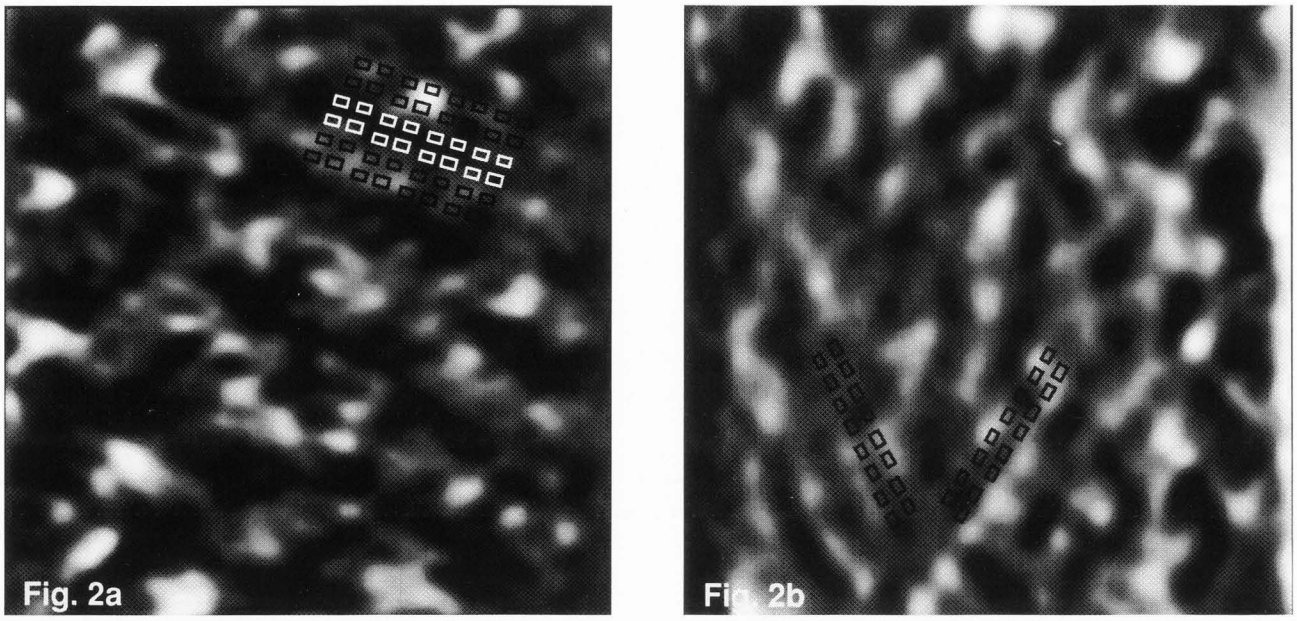

Figure 2. Structure of a bacterial S-layer prepared on a glass slide observed with a home-built SFM with optical detection at a scan size of 250 nm showing **a)** the regular lattice structure and **b)** a wedge dislocation.

reveal an oblique lattice with the parameters a = 9.4 nm, b = 7.4 nm, g = 80° (Sleytr *et al.*, 1989). Membrane fragments can be recrystallized and show the same two-dimensional lattice. This has been shown by electron microscopy on stained preparations (Pum *et al.*, 1989) and by SFM on uncoated membrane sheets that were kept in buffer solution while imaging (Ohnesorge *et al.*, 1992).

In Figure 2a the regular structure of an oblique lattice is visible. In order to form a closed envelope around the blimp-shaped bacteria cell, there have to be lattice defects especially near the poles of the cell. A so-called wedge dislocation as previously observed by electron microscopy and described in Pum *et al.* (1989), can also be seen in the SFM images (Fig. 2b).

The lattice structure appears, however, to be almost a factor of two, too large. This effect could be attributed to insufficient adhesion to the substrate or the elasticity of the cell itself combined with friction between the tip and the sample resulting in a lateral displacement that reduces the effective scan size. But this, of course, would also lead to a distortion of the angle between the lattice vectors and other image distortions. On the other hand, the lattice can be modulated such that a superstructure containing two unit cells appears, as observed on membrane fragments of this bacterial membrane (Ohnesorge *et al.*, 1992). Also, electron microscope images show a tendency to the formation of superstructures. Therefore, it seems reasonable that the dominant structure of the SFM images shows such a superstructure with twice the size of the unit cell. In Fig. 2a, in the upper right corner, every second unit cell is marked by a rectangle showing that the lattice structure derived from scattering experiments fit to the structures seen with the SFM, giving, in this way, additional information about interaction forces leading to such superstructures. A more detailed discussion on these issues is in preparation.

At the moment there is still a great deal to be learned. Nevertheless, these measurements demonstrate that the protein lattice of the bacterial cell can be imaged by SFM. The resolution is high enough for future investigations of *in situ* antigen and antibody reactions on living cells.

Structures of the erythrocyte membrane

Fig. 3a shows the erythrocyte membrane detected by the SFM at a scan size of 1 μm. The larger structures seen in this image are comparable to those observed on dried blood cells (Gould *et al.*, 1990). In all images, long linear as well as many circular ring-like structures are visible at all scales.

In experiments with Concanavalin A attached to 20 nm gold colloids, large blobs become visible. Fig. 3b shows the cell membrane before, and Fig. 3c, a few minutes after adding the gold-labeled Concanavalin A. These images demonstrate that the distribution of glycoproteins is not uniform on the cell surface.

Figure 3. SFM images with tunneling detection of erythrocyte membranes with observed corrugation amplitudes of 2-5 nm; **a)** scan size 1 μm; **b** and **c)** 300 nm x 300 nm membrane area before (**b**) adding Concanavalin A labeled with 20 nm gold colloids and the same area after (**c**) adding the Concanavalin A; **d)** before and **e)** after raising the salt concentration to 250 mM, scan size 300 nm.

Some large-scale dynamics can be seen on erythrocyte membranes by raising the salt concentration. Fig. 3d shows the cell membrane under normal conditions in a physiological salt solution, and Fig. 3e the membrane after raising the salt concentration to about 250 mM NaCl. The surface became rough on the horizontal scale

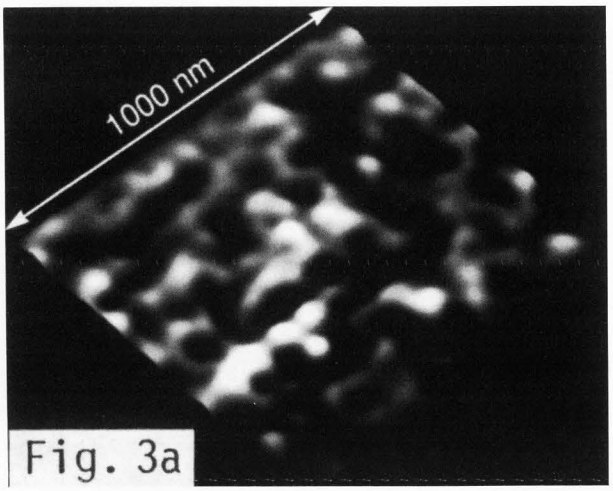

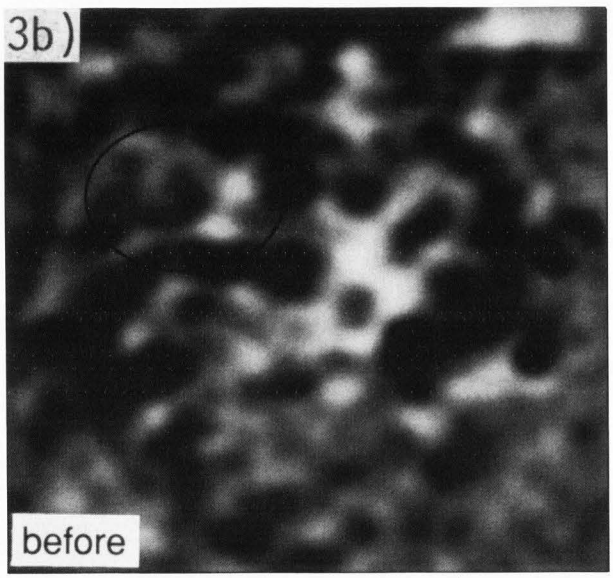

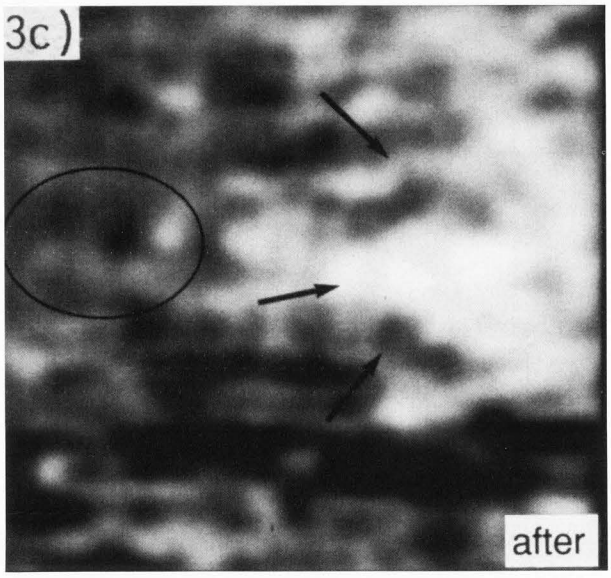

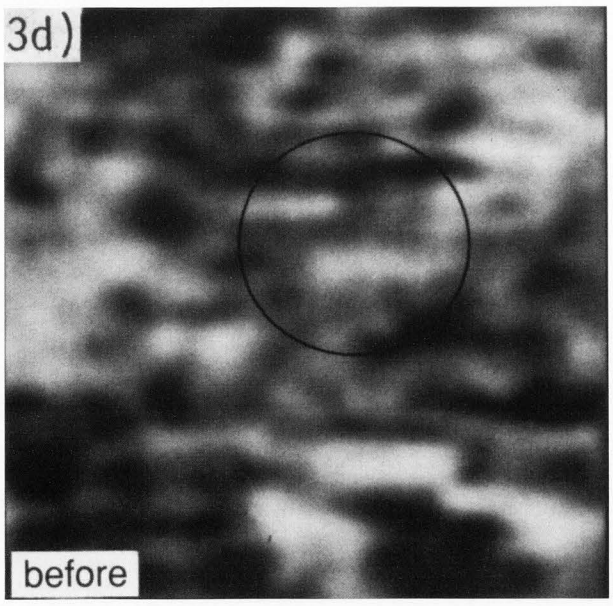

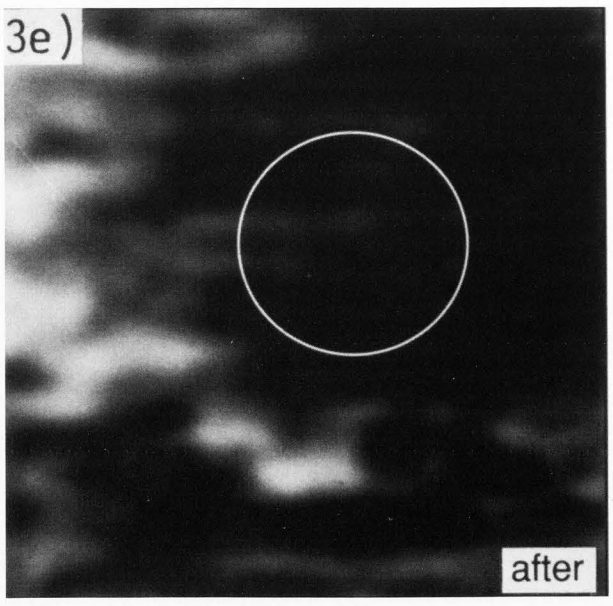

Figure 4. SFM images of surface structures of monkey kidney cells in normal growth solution observed with optical detection and compared to SEM images of such structures. **a)** areas of 1.5 μm with different loading forces between 10^{-10} N and 10^{-7} N. **b)** 3.6 μm area with obvious friction effects in the SFM image but still showing similar porous structures often found in SEM images **(c)** of virus infected cells together with virus particles. **d)** microvilli seen with the SFM **(d)** and the SEM **(e)**. **f)** 3.4 μm x 3 μm area showing beside stable structures in the right parts of the images dynamic processes on the cell surface.

---

of 100 nm, which indicates a certain folding of the membrane. The structures that are not pushed inward by the osmotic pressure are of the size and form expected for the shell structure of erythrocytes composed of 200-nm-long spectrin tetramers joined at their ends by junctional complexes of 35-nm-long actin microfilaments, which consist of an average of five spectrin fibers radiating from each complex (Darnell *et al.*, 1986).

Similar to STM, where the images are always a result of combined local spectroscopic and topographic features, the SFM images reflect topographic configurations as well as local compressibility. The linear structures in these images might, therefore, also be due to such local variations in the stiffness of the cell surface. Hence, the observed structures can reflect the cytoskeleton underneath the membrane which is a rather stiff molecular network that gives the cell its characteristic form.

Structures of cultured monkey kidney cells

The surfaces of monkey kidney cells, a cultured type used for various investigations, looks, as expected, different than those of erythrocytes. The main structures, aside from the marked folding, are reminiscent of mountain ranges. Some of the structures seen are very stable as the applied force is raised, while others tend to disappear. Some details in Figure 4a show high contrast only at high loading forces. For high loading forces the samples become more deformed depending on the local compressibility and the images become more dominated by the compressibility aspect of the imaging mechanism whereas high contrast at low loading forces, can be more closely related to topography.

The apparent shadowing of pronounced structural details in SFM images occurring particularly on strongly corrugated biological sample surfaces (i.e., 10-100 nm) is a scan direction-dependent artifact. It is caused by a phase shift in the imaging system (electronically and mechanically) when the tip has to move up or down while scanning over surface corrugations. This leads to the impression of a three-dimensional surface reconstruction with illumination in scan direction.

At this point, it should be noted that the convolution of a non-symmetric tip geometry also influences the appearance of structural details which has to be controlled by selecting well microfabricated imaging tips.

Force microscopy detects normal forces acting between the sample and the tip, and thus provides the topography information. Depending on the length of the tip, lateral forces might also deform the lever and/or the sample, and therefore, might contribute to some extent to the images (Fig. 4b). These forces can distort the image or can cause stable surface features to move or can even be so destructive that they tear off structural details (Ohnesorge *et al.*, 1992). Nevertheless, the SFM image (Fig. 4b) shows a similar porous area often seen in the scanning electron microscope (SEM) images (Fig. 4c) of infected cells surrounded by virus particles.

In the SEM and SFM images, large areas of monkey kidney epithelial cell surface are characterized by numerous finger-like longitudinal extensions, called microvilli and microplicae (Fig. 4d, e). These cytoplasmic structures make the cells' absorptive surface area 5-10 times greater than it would be otherwise. These cell surface structures are also involved in cell phagocytosis. The plasma membrane that covers these extrusions is highly specialized, and contains a surface coat of polysaccharide and enzymes. Under the plasma membrane these cells possess a cortical layer of actin filaments and actin-binding proteins that are cross-linked into a three-dimensional network closely connected to the surface membrane. These filaments have a structural role: they can pull on the membrane and create the changes seen in the SFM by means of the dynamics of the surface protrusions (Fig. 4f).

The relatively stable arrangements of the actin filaments are responsible for their relatively persistent structure. But these surface actin filaments are not permanent. During phagocytosis or cell movement, rapid changes of shape occur at the cell surface. These changes depend on the transient and regulated polymerization of cytoplasmic free actin or the depolarization during the breakdown of the actin filament complex. The time scale of cell surface changes on a larger scale observed with the SFM was about 1-2 hours at room temperature. Except for small structures some 10 nm in size, everything is quite stable for 1-2 hours. More and larger structures are rearranged only 10-15 minutes after this period has elapsed.

Fig.4a

high

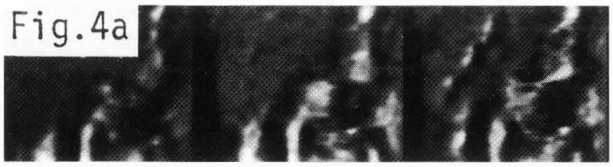

low

Fig.4b

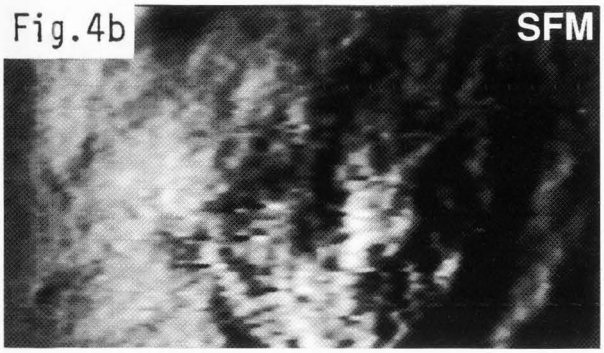

Fig.4c

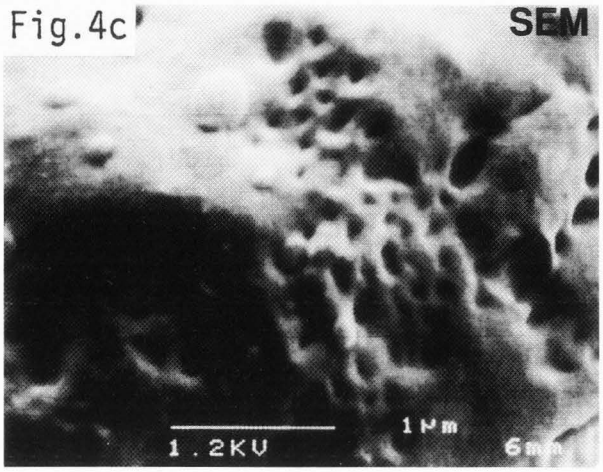

Fig.4d

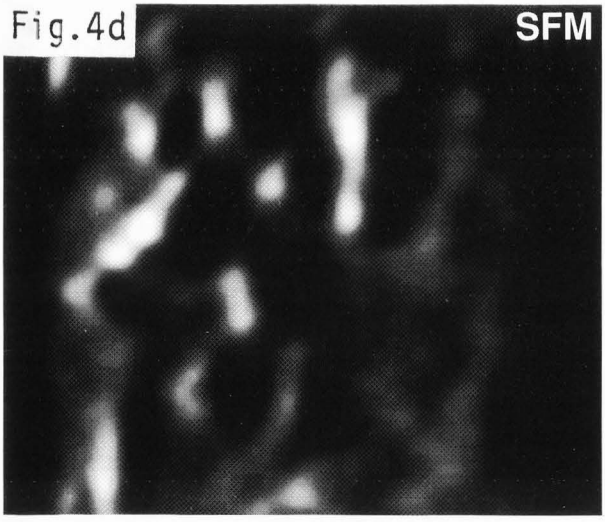

Fig.4e

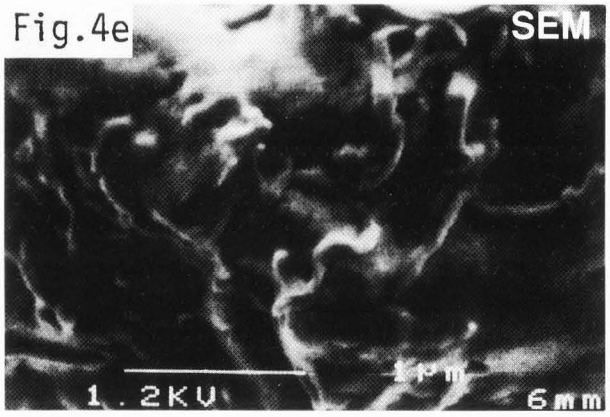

Fig.4f

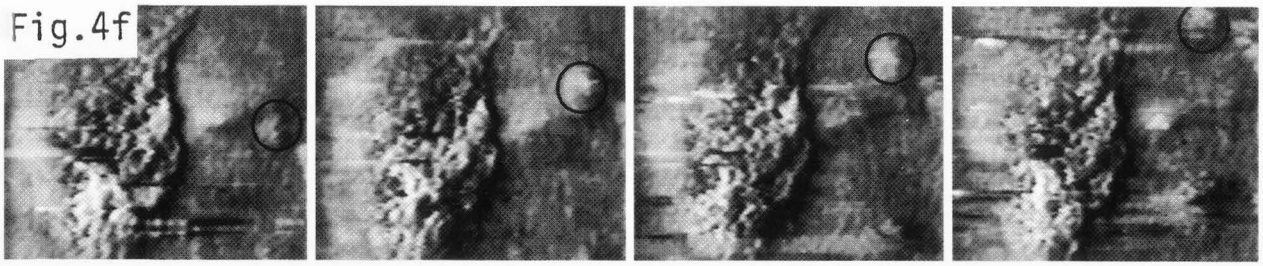

0 sec

20 sec

Figure 5. a) Exocytotic processes seen 3 hours after infection with a particle size of 50-200 nm; b) pox virus leaving the cell at the end of a microvillus, 19 hours after infection.

Surface processes on virus infected cells

With optical SFM detection it is possible to image a cell for many hours. The longest session we had with a monkey-kidney cell was 44 hours. In this experiment, we infected the cell after 2 hours of observation with vaccinia viruses and observed it until the cell finally died.

The idea to investigate virus-infected cells was that large viruses such as *pox viridae* might be of the right size to be observed easily when attacking a cell or when the progeny viruses leave the cell. We chose the vaccinia type as they are the most unlikely to infect humans. This virus is 200-300 nm in size and has quite a complex protein cover. Certain proteins are known to be responsible for its adsorption to the cell membrane without needing special binding sides. They also are involved in the penetration of the cell membrane and the disassembly of the virus to release its DNA. The reproduction of this type of virus is located in the cytoplasm.

In our experiments dealing with cells infected by viruses, we always started by observing one cell for one to two hours to determine its normal behavior and structure. The cell is kept in the normal growth solution in order to change the environment as little as possible. As we apply only light suction with the pipette, the cell is affixed quite similar to its normal growing situation. The highly concentrated viruses are kept in the same solution so that by adding them to the container in which the cell is observed by the SFM, the environment of the cell is not changed except for the virus. We add the viruses such that it takes them 2-3 minutes to reach the cell by diffusion. In our first series of eight experiments, we observed that the behavior of the cell membrane changed drastically at that point. The lever no longer detected a well-defined cell surface as the sharp onset of a repulsive force when the sample approaches the lever with a certain force. The images hardly had any contrast. This situation lasted for several minutes, in some cases only less than a minute, before the cell membrane became stiff again, even stiffer than before.

Later experiments did not confirm this effect, although we endeavored to work under identical conditions. Therefore, the dependence of this effect is not yet clear, but we consider it a worthwhile topic for a future investigation. During the 2-3 hours following infection no drastic changes were observed with our SFM, but then blobs began to form along chainlike structures and grew for several minutes before suddenly disappearing (Fig. 5a). The blobs, which are 50-200 nm, are smaller than the virus itself and may either appear and disappear again 6 or 8 times at the same place on the cell surface, or the process is seen only once.

It is known that it takes 2-3 hours for all the steps necessary before the final virus assembly can start (Moss, 1986), so we think these exocytotic processes may be connected to the reaction of the cell to the production of virus proteins or related processes. The connection to the chainlike structures supports the assumption that they belong to the stabilizing actin structures, as these are also known to be involved in transport processes at this size (Stokes, 1976).

After 6-8 hours, when the first progeny viruses are ready, the cell starts to build more microvilli, small tubes of 0.1-0.5 μm diameter and 0.5-2 μm length. These are known to be stabilized also by actin structures belonging to an internal transport system (Stokes, 1976). As Stokes showed in 1976, with electron micrographs, the virus can attach itself to this transport system and use it to leave the cell. In this case, a Golgi apparatus along the way makes a double lipid layer around the virus, enabling it to leave the cell by exocytosis in some cases through these microvilli. Stokes' images of microvilli, 20 hours after infection, show the viruses just leaving the cell (Stokes, 1976).

The structures in Fig. 5b, which we observed with the SFM, are extremely similar to the electron microscopy (EM) images by Stokes (1976). But the EM images are merely snapshots whereas with the SFM we observed the event like a movie. The exocytosis of such enveloped viruses is rather seldom; only a certain percent leave the cell in this way. With EM snapshots, one has to be lucky to fix the sample at the right moment, while with the SFM, we had to be lucky to observe the right microvillus at the right time.

Conclusions

With these studies, it is demonstrated that with a technique using basically force microscopy, the door to a new way of investigating cell surfaces locally is opened. It is possible to image the surface of living cells with a resolution of a few nanometer. The method of fixing a cell to a pipette is flexible enough to allow integration of, and combination with, well-established cell physiological techniques of manipulations used in investigations of single cells. The structures observed might be partially related to known features of membranes, but detailed structural analysis has to be left to

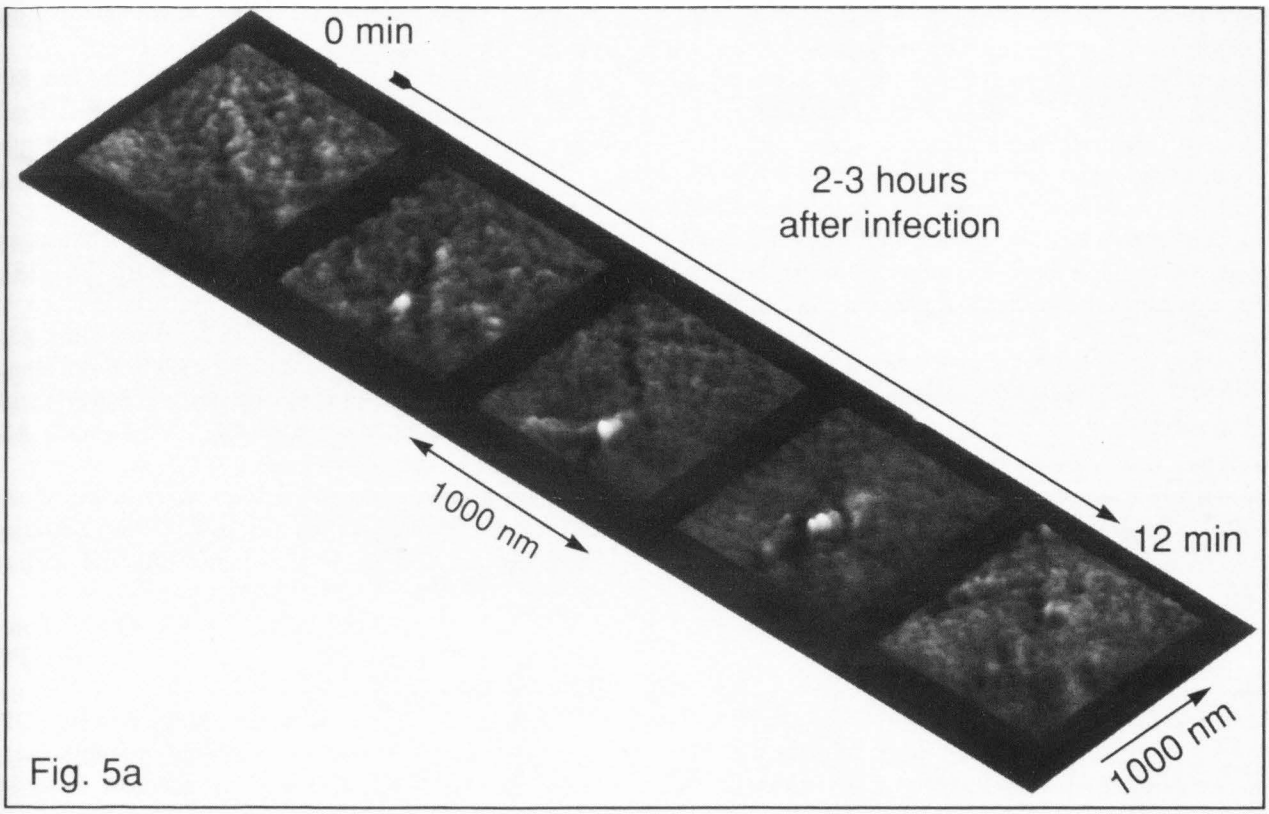
0 min
2-3 hours
after infection
1000 nm
12 min
1000 nm

Fig. 5a

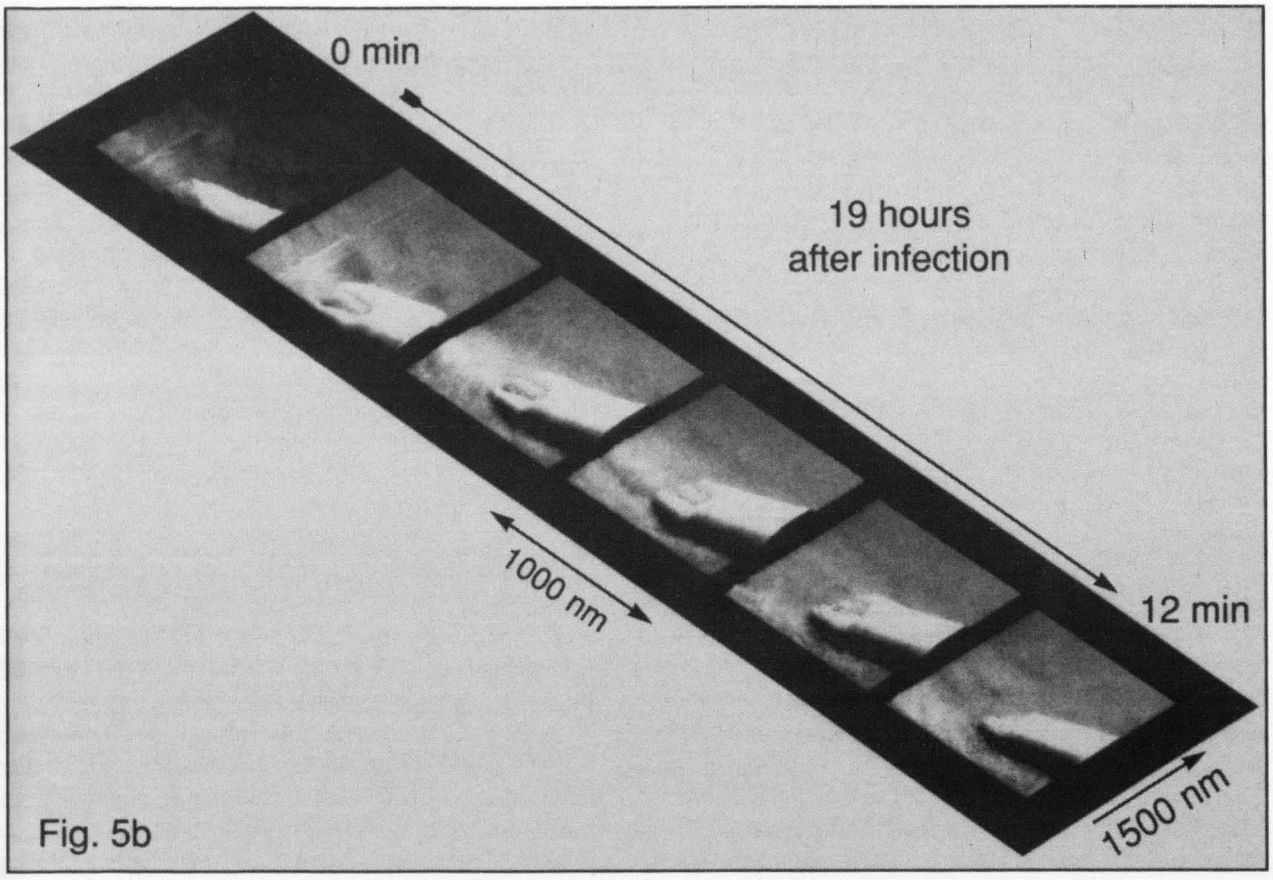
0 min
19 hours
after infection
1000 nm
12 min
1500 nm

Fig. 5b

future investigations. More important than the observations of structures with this new technique is the possibility of conducting dynamical studies of living organisms on this scale. This might give access to the observation of immune reactions, the forming of cell pores, as well as endo- and exocytosis in various cell types, the details of which are still speculative. In general, this technique makes studies of the evolution of cell membrane structures possible, and provides information that brings us closer to understanding not only the "being" of these structures, but also their "becoming".

Acknowledgments

The authors thank the Max Planck Institute for Medical Research in Heidelberg, and the WHO Collaborating Center for Collection and Evaluation of Data on Comparative Virology, Veterinärstr. 13, 8000 Munich 22, Federal Republic of Germany for supporting this work.

References

Binnig G, Rohrer H, Gerber Ch, Weibel E (1982) Surface study by scanning tunneling microscopy. Phys. Rev. Lett. **49**, 57-60.

Binnig G, Rohrer H (1984) Scanning tunneling microscopy. In: Trends in Physics 1984. Janta J, Pantoflicek J (eds.), European Physical Society, Amsterdam, 38-46.

Binnig G, Quate CF, Gerber Ch (1986) Atomic force microscope. Phys. Rev. Lett. **56**, 930-933.

Butt HJ, Wolff EK, Gould SAC, Dixon Northern B, Peterson CM, Hansma PK (1990) Imaging cells with the atomic force microscope. J. Struct. Biol. **105**, 54-61.

Czerny C-P, Mahnel H, Hornstein O (1989) Prüfung der Immunität gegen Orthopockenviren an der weiβen Maus mit Vaccinia Virus (Testing immunity against Orthopoxviruses with white mice and Vaccinia viruses). J. Vet. Med. B **36**, 100-111.

Czerny C-P, Mahnel H (1990) Structural and functional analysis of orthopoxvirus epitopes with neutralizing monoclonal antibodies. J. Gen. Virol. **71**, 2341-2352.

Dai JW, Jliao YK, Dong Q, Su YX, Lin KC (1991) The surface structure of natural membrane of macrophages in water as studied by scanning tunneling microscopy. J. Vac. Sci. Technol. **B9**, 1184-1188.

Darnell J, Lodish H, Baltimore D (1986) The plasma membrane. In: Molecular Cell Biology. Scientific American Books, New York, 569-615.

Drake B, Prater CB, Weisenhorn AL, Gould SAC, Albrecht TA, Quate CF, Cannell DS, Hansma HG, Hansma PK (1989) Imaging crystals, polymers, and processes in water with the atomic force microscope. Science **243**, 1586-1589.

Egger M, Ohnesorge F, Weisenhorn AL, Heyn SP, Drake B, Prater CB, Gould SAC, Hansma PK, Gaub HE (1990) Wet lipid-protein membranes imaged at submolecular resolution by atomic force microscopy. J. Struct. Biol. **103**, 89-94.

Fuchs H, Schrepp W, Rohrer H (1987) STM investigations of Langmuir-Blodgett films. Surf. Sci. **181**, 391-393.

Gould SAC, Drake B, Prater CB, Weisenhorn AL, Manne S, Hansma HG, Hansma PK (1990) From atoms to integrated circuit chips, blood cells, and bacteria with the atomic force microscope. J. Vac. Sci. Technol. **A8**, 369-373.

Guckenberger R, Wiegräbe W, Hillebrand A, Hartmann T, Wang Z, Baumeister W (1989) Scanning tunneling microscopy of a hydrated bacterial surface protein, Ultramicrosc. **31**, 327-331.

Häberle W, Hörber JKH, Binnig G (1989) Force microscopy on living cells. J. Vac. Sci. Technol. **B9**, 1210-1212.

Häberle W, Hörber JKH, Ohnesorge F, Smith DP, Binnig G (1992) In situ investigations of single living cells infected by viruses. Ultramicrosc. **42-44**, 1161-1167.

Hörber JKH, Lang CA, Hänsch TW, Heckl WM, Möhwald H (1988) Scanning tunneling microscopy of lipid films and embedded biomolecules. Chem. Phys. Lett. **145**, 151-154.

Hörber JKH, Schuler FM, Witzemann V, Schröter KH, Müller HG, Ruppersberg JP (1991) Imaging of cell membrane proteins with a scanning tunneling microscope. J. Vac. Sci. Technol. **B9**, 1214-1218.

Ito E, Takahashi T, Hama K, Yoshioka T, Mitzutani W, Shimizu H, Ono M (1991) An approach to imaging of living cell surface topography by scanning tunneling microscopy. Biochim. Biophys. Res. Com. **177**, 636-643.

Jericho MH, Blackford BL, Dahn DC, Frame C, MacLean D (1990) Scanning tunneling microscopy imaging of uncoated biological material. J. Vac. Sci. Technol. **B8**, 661-666.

Kasas S, Celio MR (1992) Application of scanning-probe microscopes in biology. Biophys. J. (in press).

Marti O, Ribi HO, Drake B, Albrecht TR, Quate CF, Hansma PK (1988) Atomic force microscopy of an organic monolayer. Science **239**, 50-52.

Mayr A, Bachmann PA, Bibrack B, Wittmann G (1974) Zellkulturen-Bebrütete Hühnereier-Versuchstiere (Cell cultures, incubated chicken eggs, laboratory animals). In: Virologische Arbeitsmethoden (virological working methods), Bd. I. Gustav Fischer Verlag,

Stuttgart, Germany, page 39.

Meyer E, Howald L, Overney RM, Heinzelmann H, Frommer J, Güntherodt H-J, Wagner T, Schier H, Roth S (1991) Molecular-resolution images of Langmuir-Blodgett films using atomic force microscopy. Nature **349**, 398-399.

Moss B (1986) Replication of poxviruses. In: Fundamental Virology. Fields BN, Knape DM (eds.). Raven Press, NY, 637-655.

Ohnesorge F, Heckl WM, Häberle W, Pum D, Sara M, Schindler H, Schilcher K, Kiener A, Smith DPE, Sleytr UB, Binnig G (1992) SFM studies of antibody binding to S-layers, and of protein crystals. Ultramicrosc. **42-44**, 1236-1242.

Pum D, Sara M, Sleytr UB (1989) Structure, surface charge, and self assembly of the S-layer lattice from *Bacillus coagulans* E38-66. J. Bacteriol. **177**, 5296-6001.

Ruppersberg JP, Hörber JKH, Gerber Ch, Binnig G (1989) Imaging of cell membraneous and cytoskeleton structures with a scanning tunneling microscope., FEBS Lett. **257**, 460-464.

Sakmann B, Neher E (1983) Geometric parameters of pipettes and membrane patches. In: Single-Channel Recording. Sakmann B, Neher E (eds.), Plenum Press, New York, 37-51.

Sleytr UB, Messner P (1989) Self assembly of crystalline bacterial cell surface layers (S-layers). In: Electron Microscopy of Subcellular Dynamics. Plattner H (ed.), CRC Press, Boca Raton, Florida, 13-31.

Smith DPE, Bryant A, Quate CF, Rabe JP, Gerber Ch, Swalen JD (1987) Images of a lipid bilayer at molecular resolution by scanning tunneling microscopy. Proc. Natl. Acad. Sci. USA **84**, 969-972.

Stemmer A, Reichelt R, Engel A, Rosenbusch JP, Ringger M, Hidber HR, Güntherodt H-J (1987) Scanning tunneling and scanning transmission electron microscopy of biological membranes. Surface Science **181**, 394-402.

Stokes GV (1976) High-voltage electron microscope study of the release of vaccinia virus from whole cells. J. Virol. **18**, 636-643.

Travaglini G, Rohrer H, Amrein M, Gross H (1987) Scanning tunneling microscopy on biological matter. Surf. Sci. **181**, 380-390.

Worcester DL, Miller RG, Bryant PJ (1988) Atomic force microscopy of purple membranes. J. Microsc. **152**, 817-821.

Zasadzinski JAN, Schneir J, Gurley J, Elings V, Hansma PK (1988) Scanning tunneling microscopy of freeze-fracture replicas of biomembranes. Science **239**, 1013-1015.

Discussion with reviewers

A.L. Weisenhorn: Are the vertically (Fig. 2a) and horizontally (Fig. 2b) oriented structure not also due to the tip shape and/or filtering?

Authors: This is indeed something one has to keep in mind, and therefore, should not make conclusions from a single experiment. The structures seen are, however, very similar for imaging with various different tips and we are confident that they correspond to the sample. These structures are visible in the raw data as well, and are reproducible in many images. Only lowpass filtering to reduce high frequency noise has been carried out. A Fourier transformation shows the corresponding peaks, but we decided not to include such an image in this paper, because we think that an interpretation of what is detected with an SFM tip on such structures should be done in more detail by comparing images of different lattice structures.

A.L. Weisenhorn: Regarding the interpretation of the lost contrast after infection: Could a change in optical density (due to temperature or salt concentration difference or ...) not also change the contrast for some time until the solution comes to a stable state again?

Authors: The viruses are suspended in the same medium as the cell during the experiment. As both solutions are kept at room temperature there should be only a difference in having viruses in the solution or not, and in a 10% change of the solution volume. The effect of the changing volume was checked with pure solution, and changes in the SFM imaging were not observed. The small amount of viruses in the minimal growth medium also should not alter the composition of this solution or of the optical density significantly.

R. Reichelt: Scanning of the capillary with the cell attached generate frictional forces on both the capillary and the cell due to viscosity of the solution. That frictional force depends on the shape of the sample, the viscosity of solution, the scanning speed and its direction as well. To what extend the frictional forces may affect the shape and the position of the cell attached to the capillary, hence creating distortions in the SFM image of the cell surface? The strongest influence I expect at the points where the scanning direction is changed.

Authors: For successful imaging the cells have to be properly fixed to the pipette. In this case, we do not see any effect of friction due to viscosity. With high optical magnification, we do not observe any reduction in the scanning width when the scanning frequency is changed by orders of magnitudes within the range used in our experiments. The same is true for the SFM images. By reducing the scanning frequency, e.g., by one order of

magnitude the results are the same. Friction between tip and sample appears to be a more serious problem.

R. Reichelt: A frictional force between tip and sample is assumed to cause lateral displacement that reduces the effective scan size. Obviously that displacement is different in x- and y- direction in Fig. 2a thus changing the angle between the lattice vectors. Did you try (i) to reproduce that finding at different areas at the cell surface, and (ii) to record a second micrograph after rotation of the scan direction by 90°? The latter could be helpful to quantify the distortion. Please comment on this.
Authors: We just wanted to mention the possibility of reducing the effective scan size by various lateral force effects. However, distortions of that kind are usually accompanied by strong distortions at the edges of the image and vary strongly with changed scanning direction, loading force and/or scanning speed. This is not true for the images shown, as we imaged with rotated scan directions, changed scanning speeds, and on different preparations at several places. The point we wanted to make is that SFM results are a convolution of local topography, compressibility and also of local friction. Our consideration was that possibly the superimposed structure might be due to local compressibility or local friction if every second molecule responds differently in this respect. Electron microscopy might not be sensitive enough to such an effect, if these effects are dependent on the environment or on minor differences in topography.

H.J. Butt: If features can appear larger than they are, how reliable are the other figures? The bacteria are relatively rigid structures compared to the mammalian cells; distortions caused by friction should be smaller on bacteria. Is the scaling on images of mammalian cells even less reliable?
Authors: As mentioned before: i) reduced effective scan size can possibly occur but they can be recognized by other effects. Edge effects in our cell experiments are normally quite small and the images show only little variations when loading force or scan speed considerably are changed. ii) The structures on the bacterial cell are not too small, but belong to a superstructure formed by groups of unit cells. This effect is also detected with the EM and on membrane preparations with the SFM. iii) The structures seen with the SFM correspond quite well to what is known from EM images. They are not just single events documented in single pictures. We have many video tapes where these structures, their dynamics, and their evolution is documented continuously over hours, in one case, with monkey kidney cells over two days.